Electrochimica Acta 67 (2012) 166–171

Contents lists available at SciVerse ScienceDirect

Electrochimica Acta

journal homepage: www.elsevier.com/locate/electacta

TiO_2 nanoparticles promoted Pt/C catalyst for ethanol electro-oxidation

Lihong Yu[a], Jingyu Xi[b,*]

[a] Department of Chemistry, The University of Hong Kong, Pokfulam Road, Hong Kong, China
[b] Lab of Advanced Power Sources, Graduate School at Shenzhen, Tsinghua University, Shenzhen 518055, China

ARTICLE INFO

Article history:
Received 28 November 2011
Received in revised form 5 February 2012
Accepted 7 February 2012
Available online 15 February 2012

Keywords:
Direct ethanol fuel cells
Ethanol electro-oxidation
Pt/C catalysts
TiO_2 nanoparticles
Composite anode catalysts

ABSTRACT

A simple and efficient method to enhance the activity of Pt/C catalysts for direct ethanol fuel cells (DEFCs) by ultrasonically mixing commercial Pt/C catalyst and TiO_2 nanoparticles is reported. In this novel composite anode catalyst, the as-prepared TiO_2 nanoparticles are dispersed homogeneously in the interspaces of Pt based C nanoparticles, resulting in a great deal of TiO_2-Pt-C interfaces, which greatly accelerate the ethanol electro-oxidation reaction. Cyclic voltammetry (CV), CO stripping, chronoamperometry and electrochemical impedance spectroscopy (EIS) measurements confirm that this composite catalyst structure has excellent activity and stability toward ethanol and CO electro-oxidation compared to the pure Pt/C catalyst. Particle size and content of TiO_2 are also discussed with respect to effect on catalyst performance.

1. Introduction

Direct alcohol fuel cells (DAFCs) are very attractive nowadays as power sources for mobile and portable applications [1–3]. Consequently, oxidation of small organic molecules has been studied extensively over the past several decades. In DAFCs, ethanol has its unique advantages and proves to be a promising option as fuel due to its high energy density and environmental friendship [4]. It can be produced in large quantities from the fermentation of biomass and both ethanol and its final oxidation product, carbon dioxide, are relatively non-toxic. Platinum is generally considered to be the best monometallic catalyst for the electro-oxidation of small organic molecules. Therefore, most studies focused on platinum-based catalysts and many achievements typically in elucidating the reaction mechanism, identifying the intermediates, and enhancing the catalyst activity have been obtained [5–15]. However, the price of Pt is high and its superior catalytic activity drops severely with time when traces of carbon monoxide are present due to poisoning effect caused by CO-like species [15,16]. In recent years, efforts have been made to minimize the use of precious metal by introducing some other kinds of metal into the catalyst such as Pt-based binary (PtRu, PtSn, etc.) [17–19], ternary (PtRuNi, PtRuIr, etc.) [20,21] and quaternary (PtRuOsIr, etc.) [22], and diminish the CO poisoning effect by introducing some metal oxides into the catalyst such as CeO_2 [16], SnO_2 [23], RuO_2 [13] and ZrO_2 [24], etc. For example, Cao et al. [13] recently reported a novel nano-composite Pt/RuO_2·H_2O/CNT catalyst which showed excellent performance compared with the benchmark PtRu/C catalyst. Scibioh et al. [25] reported a Pt–CeO_2/C anode catalyst for direct methanol fuel cells replacing Ru by CeO_2 in PtRu/C catalyst. The above referred metal oxides have received considerable attention for they all have fluorite structure whose cations can switch between +3 and +4 oxidation states and have the ability to act as an oxygen buffer [26] which is involved in promoting the CO removal from Pt during the electro-oxidation [25].

Semiconductor TiO_2 has large band gap which can also serve as oxygen buffer and is already proved an effective photocatalyst to carry out methanol oxidation under UV excitation [27]. In fact, Kamat and co-workers [27] also found that TiO_2 can improve the performance of the Pt–Ru catalyst for methanol oxidation without UV excitation, namely in darkness, by diminishing CO poisoning effects. In this paper we explored the effect of TiO_2 nanoparticles in the aspect of removing CO from Pt surface and revealed a simple and efficient method to enhance the activity of Pt/C catalysts for direct ethanol fuel cells (DEFCs) by ultrasonically mixing commercial Pt/C catalyst and TiO_2 nanoparticles. In the meanwhile, the effect of TiO_2 particle size and content on catalyst performance was investigated.

2. Experimental

2.1. Synthesis and characteristics

All the reagents used in this study are of analytical grade if not specified. For the synthesis of TiO_2 nanoparticles, $K_2C_2O_4$ solution was added drop-wise with constant stirring into the tetrabutyl

* Corresponding author. Tel.: +86 755 26036181; fax: +86 755 26036181.
E-mail address: xijingyu@gmail.com (J. Xi).

0013-4686/$ – see front matter © 2012 Elsevier Ltd. All rights reserved.
doi:10.1016/j.electacta.2012.02.020

titanate solution maintaining a pH value of 10. The resultant precipitation was filtrated and washed with deionized water and ethanol repeatedly, and then dried at 80 °C for 12 h. This precipitation and KNO_3 were mixed efficiently in a mortar at a molar ratio of 1:3. The mixture was calcined at 500 °C for 3 h, and then cooled to ambient temperature. The product was immersed in deionized water, washed and filtered repeatedly to remove the residual fluxes. Finally, the product was dried at 120 °C to obtain the TiO_2 nanoparticles (denoted as as-prepared TiO_2) with the the BET surface area of 136.8 m^2/g. Degussa P25 TiO_2 nanoparticles of 80% anatase and 20% rutile with high purity (denoted as P25) were used as commercially received with the the BET surface area of 54.2 m^2/g. The morphologies of the TiO_2 nanoparticles, Pt/C catalyst and Pt/C + TiO_2 composite catalyst were examined by transmission electron microscope (TEM, JEOL model JEM-1200EX) and scanning electron microscope (SEM, LEO1530) in which EDS analysis was used to analyze the element distribution in the catalyst architecture. The structure of TiO_2 nanoparticles was examined by X-ray diffraction (XRD) analysis using the Rigaku X-ray diffractometer with Cu Kα-source. The 2θ angular region between 20° and 80° was explored at a scan rate of 6° min^{-1} with step of 0.02°.

2.2. Working electrode preparation

The Pt/C catalyst ink was prepared by mixing the Pt/C catalyst (E-Tek, 20 wt.% Pt) with perfluorsulfonic acid solution (5 wt.%, Nafion®, DuPont), ethylene glycol (EG) and deionized water ultrasonically. For the case of Pt/C + TiO_2 catalyst ink, TiO_2 nanoparticles were first dispersed in deionized water ultrasonically, and then mixed with Pt/C, Nafion®, and EG ultrasonically. The resulting slurries were spread onto gold patches of ca. 1.0 cm^2 (1 cm × 1 cm). Then the electrodes were dried at 80 °C in air with the catalyst loadings of about 0.1 mg Pt/cm^2.

2.3. Electrochemical measurements

Electrochemical measurements were carried out in a three-electrode cell using a Solartron SI1287/1255B workstation at 25 °C. A saturated calomel electrode (SCE) and Pt gauze were used as reference and counter electrodes, respectively. All electrode potentials in this paper were referred to the SCE. A solution of 1 M ethanol + 1 M $HClO_4$ was used as electrolyte. Several activation scans were performed until reproducible voltammograms were obtained. Cyclic voltammograms (CV) were recorded from −0.2 to 1.0 V at a scan rate of 50 mV/s. The oxidation of pre-adsorbed CO was measured by CO stripping voltammetry in 1 M $HClO_4$ solution at a scan rate of 10 mV/s. All the currents in this paper are specific currents (i) normalized to mass of Pt. The experimental error in voltage measurements during CV test in this work was within 5 mV. Electrochemical impedance spectroscopy (EIS) was carried out for the Pt/C, Pt/C + 20 wt.%TiO_2, and Pt/C + 20 wt.%P25 catalysts at 0.45 V in a solution of 1 M ethanol + 1 M $HClO_4$ with a frequency range from 1 MHz to 0.5 Hz.

3. Results and discussion

3.1. Morphological characterization and proposed mechanism

Fig. 1 shows the XRD pattern of as-prepared TiO_2 nanoparticles and all the sharp peaks can be indexed to the anatase TiO_2 which means that the structure of the as-prepared TiO_2 nanoparticles is uniformly anatase.

Fig. 2(a) and (b) shows the TEM images of as-prepared TiO_2 nanoparticles and Pt/C (E-Tek, 20 wt.% Pt) catalyst, respectively. The carbon nanoparticles have an average size of about 30 nm while TiO_2 nanoparticles have an average size of about 10 nm. Fig. 2(c) shows the SEM image of the as-prepared catalyst architecture of Pt/C + 20 wt.%TiO_2, with the inset showing the enlarged part. In order to reveal the actual architecture of catalyst in the electrode, the SEM sample was made through the same procedure as the working electrode preparation except that the resulting slurry was spread onto the SEM supporter. Fig. 2 (d) and (e) shows the element distribution positions of Ti (from TiO_2) and Pt (from Pt/C) for the selected position in Fig. 2 (c) by EDS. It can be seen that the distribution of elements Pt and Ti is homogeneous in the catalyst architecture which means that Pt/C nanoparticles and TiO_2 nanoparticles can be dispersed evenly in the catalyst system by ultrasonically mixing. This can result in a great deal of TiO_2–Pt–C interfaces and may promote the electro-oxidation of adsorbed CO species on Pt surface, as demonstrated in Fig. 2(f).

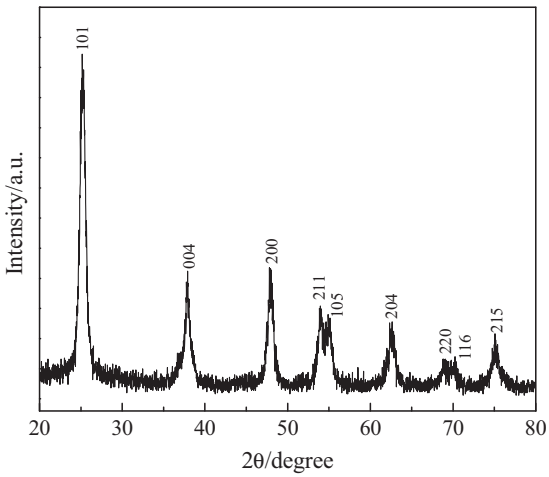

Fig. 1. XRD pattern of as-prepared TiO_2 nanoparticles.

Fig. 2(f) shows the schematic diagram of structure of Pt/C + TiO_2 catalyst. The right part shows the mechanism of CO oxidation at the interfaces of TiO_2/Pt. Kamat et al. [27] have proved that TiO_2 improves the performance of the Pt-Ru catalyst in darkness, indicating possible surface area improvement or diminished poisoning effects. In our experiments, there is no obvious improvement of surface area of Pt through adding TiO_2. The electrochemically active surface (EAS) of Pt is 58.5 m^2/g and 61.2 m^2/g before and after adding TiO_2. An EAS improvement of 4.6% may not account for more than a 50% improvement of ethanol oxidation current from 412.3 mA/mg Pt to 647.6 mA/mg Pt before and after adding TiO_2 as shown in Fig. 3(a). Data in Fig. 3(a) will be discussed in more detail later. It is well known that in fuel cells some oxides such as SnO_2 [28], RuO_2 [13], TiO_2 [29] can promote the CO removal and improve the catalyst activity by supplying active oxygen species. This encourages us to investigate the relationship between the big improvement of ethanol oxidation current and the TiO_2-accelerated oxidation of CO species. Detailed intermediates and sub-products (such as acetaldehyde and acetic acid) are not discussed here since reaction mechanism of ethanol electro-oxidation involves several steps and products from Ethanol oxidation still remain a great challenge [30].

3.2. Cyclic voltammetry and chronoamperometry analysis

Fig. 3(a) shows CV curves of ethanol electro-oxidation on Pt/C catalyst and Pt/C + 20 wt.%TiO_2 catalyst, while Fig. 3(b) shows the stability of Pt/C + 20 wt.%TiO_2 catalyst for ethanol electro-oxidation. It can be seen from Fig. 3(a) that ethanol oxidation on Pt/C + 20 wt.%TiO_2 catalyst has higher electro-catalytic current than on Pt/C catalyst over the whole scanning voltage range. Correspondingly, the peak current of ethanol oxidation on

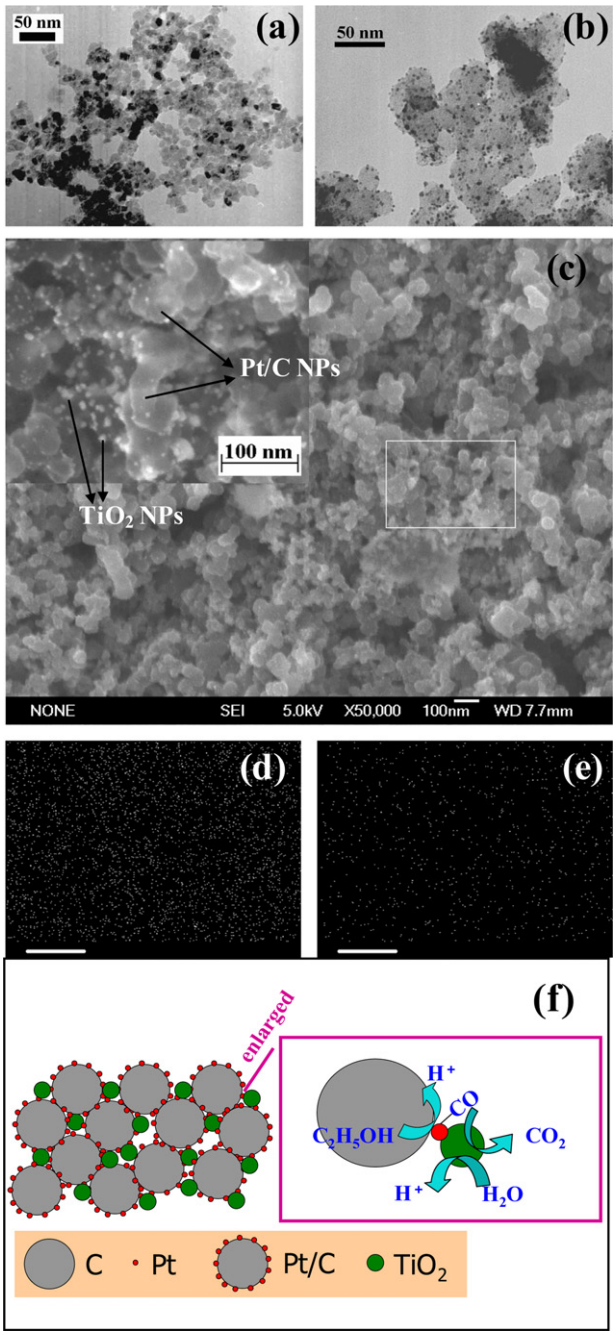

Fig. 2. (a) TEM image of as-prepared TiO_2 nanoparticles. (b) TEM image of Pt/C (E-Tek, 20 wt.% Pt) catalyst. (c) SEM image of the catalyst architecture of Pt/C + 20 wt.%TiO_2, Inset shows the enlarged SEM image. (d) and (e) element distribution image of Ti (from TiO_2) and Pt (from Pt/C) of the selective position in (c), measured by EDS. Scale bar: 100 nm. (f) Schematic diagram of structure of Pt/C + 20 wt.%TiO_2 catalyst. The right part shows the mechanism of CO oxidation at the interfaces of TiO_2-Pt/C (Nafion ionomer is not shown in this figure).

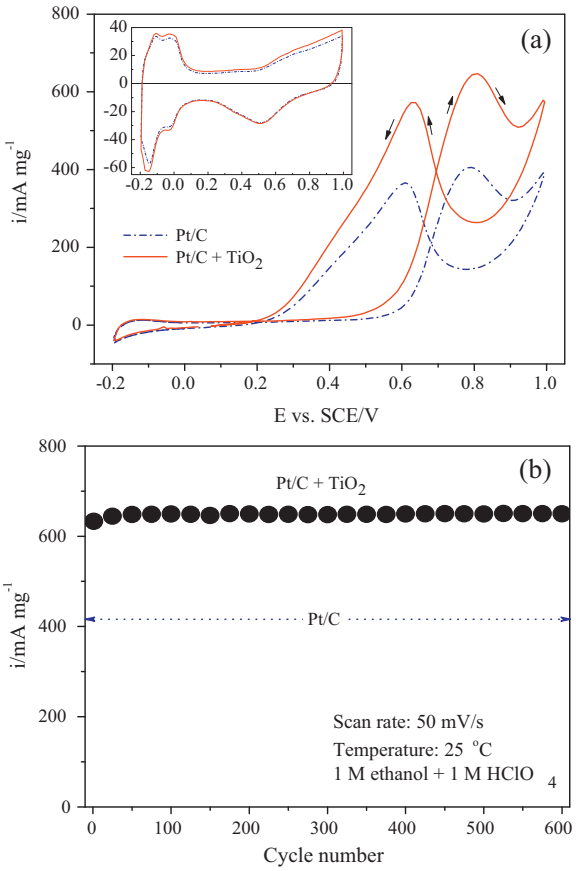

Fig. 3. (a) CV curves of ethanol electro-oxidation on Pt/C and Pt/C + 20 wt.%TiO_2 catalysts at 25 °C in 1 M ethanol + 1 M $HClO_4$ with a scan rate of 50 mV/s (only the 50th scan is shown and used for comparison of the catalytic activity of the specified catalysts). Specific current *i* is for the current normalized to mass of Pt. Inset shows the CV curves without ethanol. (b) Stability of the Pt/C + 20 wt.%TiO_2 catalyst over 600 cycles of ethanol electro-oxidation.

Pt/C + 20 wt.%TiO_2 catalyst is 647.6 mA/mg Pt much higher than on Pt/C catalyst 412.3 mA/mg Pt. The onset potential of ethanol oxidation on Pt/C + 20 wt.%TiO_2 catalyst is 0.38 V lower than on Pt/C catalyst 0.46 V. These results indicate that Pt/C + 20 wt.%TiO_2 catalyst has better electro-catalytic activity for ethanol oxidation than Pt/C does. In addition, as shown in Fig. 3(b), there is almost no activity degradation observed for Pt/C + 20 wt.%TiO_2 catalyst even after 600 cycles of uninterrupted scanning in 1 M ethanol + 1 M $HClO_4$ solution, implying the good stability of Pt/C + 20 wt.%TiO_2 composite catalyst in acid medium. Importantly, from the H_2 adsorption–desorption region of the CV curves in Fig. 3(a) insert we can get the EAS of Pt 61.2 m^2/g for Pt/C + 20 wt.%TiO_2 catalyst, very close to 58.5 m^2/g for Pt/C catalyst. Such a result indicates that TiO_2 promoting the electro-oxidation of ethanol on Pt/C + TiO_2 catalyst may be not due to increasing EAS of Pt, and instead may be due to diminishing CO poisoning effect.

As the CO species are the main poisoning intermediate during ethanol electro-oxidation, a good catalyst should possess excellent CO electro-oxidation ability, which can be verified by CO stripping test. Fig. 4 shows CO stripping curves for Pt/C catalyst in (a), for Pt/C + 20 wt.%TiO_2 catalyst in (b), and for pure TiO_2 nanoparticles in (c). From Fig. 4(a) and (b), significant differences between the onset potentials of CO oxidation for Pt/C + 20 wt.%TiO_2 catalyst and Pt/C catalyst are observed. The onset potential for CO oxidation on Pt/C + 20 wt.%TiO_2 catalyst is lower (0.42 V) than that on Pt/C catalyst (0.51 V). The CO oxidation peak potential on Pt/C + 20 wt.%TiO_2 catalyst (0.51 V) is also lower than that on Pt/C catalyst (0.59 V). According to the oxidization effect of TiO_2, the CO species on the Pt/TiO_2 interfaces are transformed to CO_2, releasing the active sites on Pt for further electrochemical reaction, and hence, the ethanol electro-oxidation is greatly enhanced. In addition, there is a very small CO oxidation current peak at about 0.30 V on Pt/C + 20 wt.%TiO_2 catalyst (see Fig. 4(b) enlargement), which may be attributed to the direct CO oxidation on the surface of TiO_2. This can be confirmed by the CO stripping voltammetry result on pure TiO_2 nanoparticles as shown in Fig. 4(c), where the CO stripping current on pure TiO_2 nanoparticles also occurs around

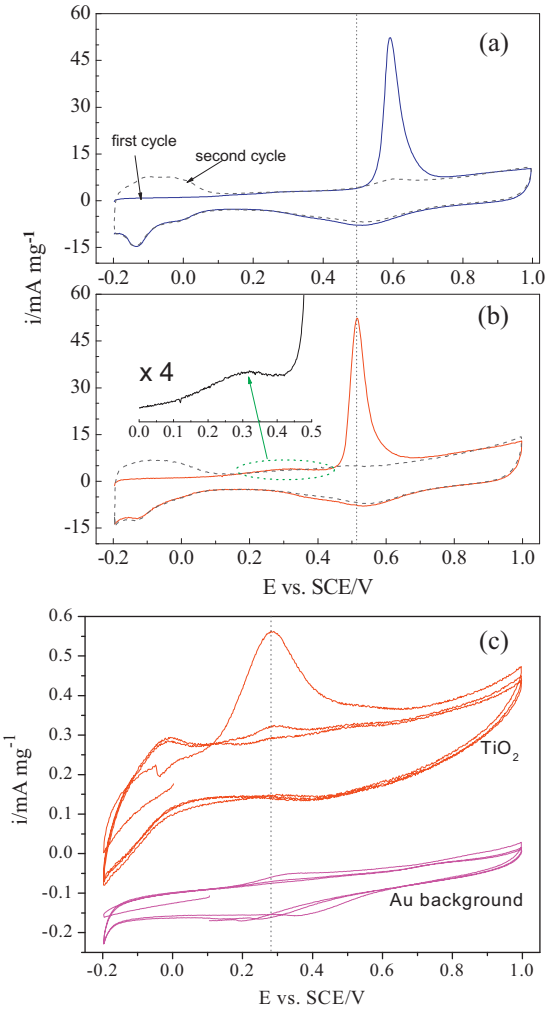

Fig. 4. (a) & (b) CO stripping curves at 25 °C in 1 M $HClO_4$ with a scan rate of 10 mV/s for Pt/C and Pt/C + 20 wt.% TiO_2 catalysts, specific current i is for the current normalized to mass of Pt. (c) CO stripping curves for TiO_2 nanoparticles and gold patch respectively in 1 M $HClO_4$ with a scan rate of 10 mV/s at 25 °C, specific current *i* is for the current normalized to mass of TiO_2 and Au respectively. CO was adsorbed at 0.1 V for 20 min, and then unadsorbed CO was removed by N_2 bubbling for 30 min at 0.1 V.

0.30 V. It is noticed that the current is quite small and this may be explained by the weak CO adsorption on the surface of TiO_2. The big decrease of CO stripping potential on Pt/C + 20 wt.%TiO_2 catalyst compared to Pt/C catalyst make us further believe that TiO_2 improves the ethanol oxidation very likely by diminishing CO poisoning effect.

Fig. 5 shows the chronoamperometry curves of CO oxidation on Pt/C and Pt/C + 20 wt.%TiO_2 catalysts at 0.50 V and 0.45 V, respectively. For both potentials, the CO oxidation peak time for Pt/C + 20 wt.%TiO_2 catalyst is obviously shorter than that for pure Pt/C catalyst, suggesting a faster CO oxidation kinetics at Pt/C + 20 wt.%TiO_2 catalyst, which is another evidence that TiO_2 plays an important role to enhance the performance of Pt/C catalyst.

Fig. 6 shows the chronoamperometry curves for the electro-oxidation of ethanol on Pt/C and Pt/C + 20 wt.%TiO_2 catalysts at 0.5 V. Although the currents are decayed for both catalysts, the initial and limiting currents of Pt/C + 20 wt.%TiO_2 catalyst keeps higher than those of Pt/C catalyst throughout all the range under the same experimental conditions. This further confirms that the composite Pt/C + 20 wt.%TiO_2 catalyst is more active than the pristine Pt/C catalyst for ethanol electro-oxidation.

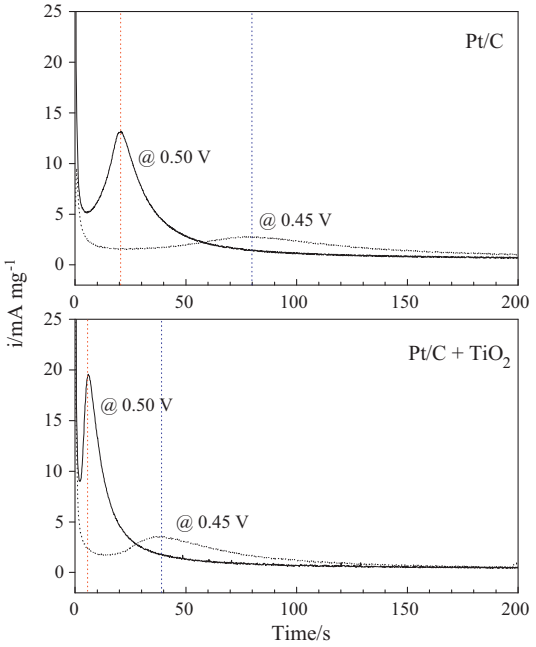

Fig. 5. Chronoamperometry curves of CO adlayer oxidation on Pt/C and Pt/C + 20 wt.% TiO_2 catalysts in 1 M $HClO_4$ at different potentials at 25 °C. Specific current i is for the current normalized to mass of Pt. CO was adsorbed at 0.1 V for 20 min, and then unadsorbed CO was removed by N_2 bubbling for 30 min at 0.1 V.

3.3. *Effect of TiO_2 particle size and content on catalyst performances*

In order to reveal the influence of TiO_2 particle size on the performance of the catalyst, we compared the catalysis activity of Pt/C, Pt/C + 20 wt.%TiO_2 and Pt/C + 20 wt.%P25 catalysts. P25 is a kind of famous TiO_2 nanoparticles made by Degussa and has an average particle size of about 30 nm. Fig. 7 shows the TEM image of Degussa P25 TiO_2 nanoparticles in (a) and the SEM image of the catalyst architecture of Pt/C + 20 wt.%P25 in (b). The SEM sample was also made imitating the working electrode preparation process. The inset between (a) and (b) shows the schematic representation for the catalyst structure of Pt/C + 20 wt.%P25. It can be seen that the particle size of P25 is much bigger than the as-prepared TiO_2 and similar to C support used in this paper (see Fig. 7(b)). As a result, it is not possible for P25 to be located in the interspaces of Pt/C like the case of as-prepared TiO_2 nanoparticles.

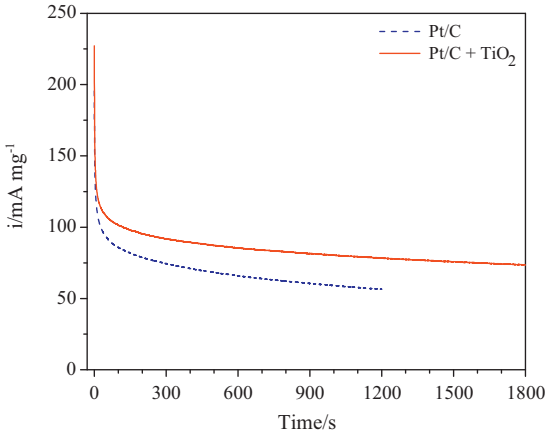

Fig. 6. Chronoamperometry curves for ethanol electro-oxidation on Pt/C and Pt/C + 20 wt.% TiO_2 catalysts in 1 M ethanol + 1 M $HClO_4$ at 0.5 V vs. SCE. Specific current *i* is for the current normalized to mass of Pt.

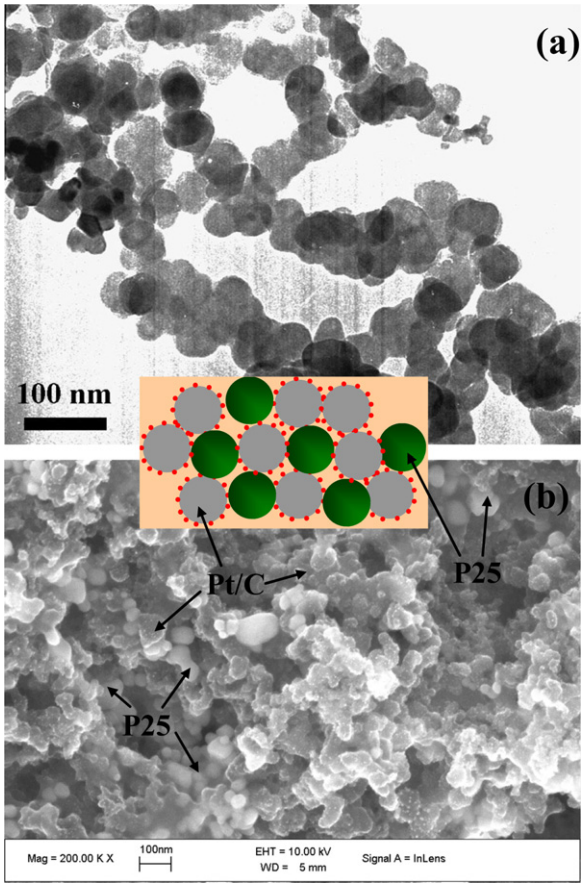

Fig. 7. (a) TEM image of Degussa P25 TiO_2 nanoparticles. (b) SEM image of the catalyst architecture of Pt/C + 20 wt.% P25. The inset between (a) and (b) shows schematic diagram for the catalyst structure of Pt/C + 20 wt.%P25.

Fig. 8 shows the CV curve of ethanol electro-oxidation on Pt/C + 20 wt.%P25 catalyst in (a), schematic diagram for how TiO_2 particle sizes affect the catalyst activity in (b), and Nyquist plots of Pt/C, Pt/C + 20 wt.%TiO_2, and Pt/C + 20 wt.%P25 catalysts in (c). From the CV curve in Fig. 8(a), we can see that the peak current of ethanol electro-oxidation on Pt/C + 20 wt.%P25 catalyst is 407.6 mA/mg Pt, much lower than that (647.6 mA/mg Pt) on Pt/C + 20 wt.%TiO_2 catalyst and even no better than that (412.3 mA/mg Pt) on pristine Pt/C catalyst. The onset potential of ethanol oxidation on Pt/C + 20 wt.%P25 catalyst is 0.45 V, much higher than that (0.38 V) on Pt/C + 20 wt.%TiO_2 catalyst and near to that (0.46 V) on pristine Pt/C catalyst. The EAS of Pt in Pt/C + 20 wt.%P25 catalyst is 57.2 m^2/g, calculated from the H_2 adsorption–desorption region of CV curve in inset of Fig. 8(a), lower than that in Pt/C + 20 wt.%TiO_2 catalyst and Pt/C catalyst.

In order to demonstrate more clear how the TiO_2 particle size affects the catalyst activity, we draw a sketch map including three typical conditions of TiO_2 particle size as shown in Fig. 8(b). TiO_2 nanoparticles can improve the ethanol oxidation by diminishing CO poisoning effect resulting in improved Pt utilization. However, TiO_2 has bad electron conductivity. When there is no TiO_2 in the catalyst, although the catalyst gets no improvement in Pt utilization, it gets good electron conductivity. When there is a certain amount of TiO_2 nanoparticles of proper size (e.g. 10 nm) added evenly, we obtain a high Pt utilization and good electron conductivity, and thus get an improvement of more than 50% in terms of ethanol oxidation peak current. However, when the TiO_2 particle (e.g. P25) is as big as the C particles in the catalyst, it can't locate in the interfaces of the Pt/C particles like as-prepared TiO_2, the catalyst

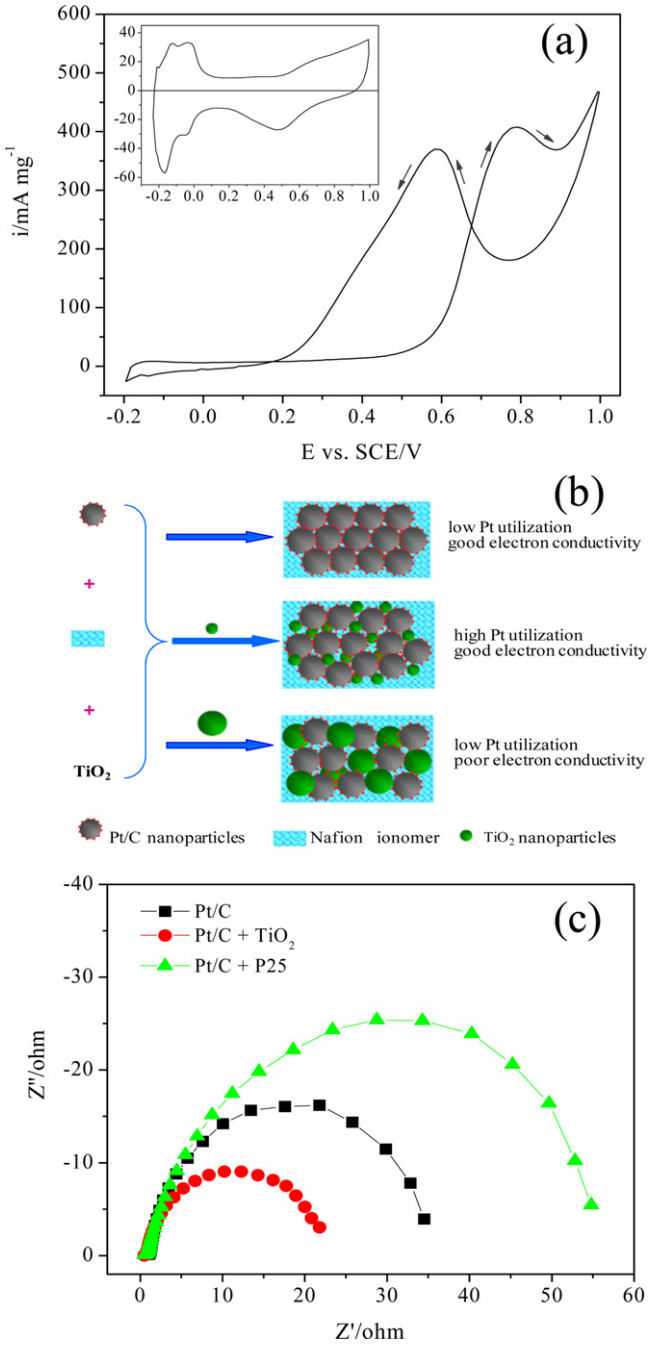

Fig. 8. (a) CV curve of ethanol electro-oxidation on Pt/C + 20 wt.%P25 catalyst in 1 M ethanol + 1 M $HClO_4$ with a scan rate of 50 mV/s at 25 °C. Specific current i is for the current normalized to mass of Pt. Inset shows the CV curve without ethanol. (b) Schematic diagram for how TiO_2 particle sizes affect the catalyst activity. (c) Nyquist plots of Pt/C, Pt/C + 20 wt.% TiO_2, and Pt/C + 20 wt.% P25 catalysts at 0.45 V vs. SCE in 1 M ethanol + 1 M $HClO_4$.

activity is decelerated instead of accelerated. The above reasoning can be verified by electrochemical impedance spectroscopy (EIS) measurement, as shown in Fig. 8(c). The diameter of the semicircle arc is a measure of charge transfer resistance (Rct) related to the charge transfer reaction kinetics [31,32]. It shows a significant decrease of Rct for Pt/C + 20 wt.%TiO_2 catalyst and an increase of Rct for Pt/C + 20 wt.%P25 catalyst indicating the charge transfer accelerated for the former and decelerated for the latter compared to the pristine Pt/C catalyst. This result has good coherence with the CV curves of ethanol electro-oxidation on Pt/C, Pt/C + 20 wt.%TiO_2, and Pt/C + 20 wt.%P25 catalysts (see Figs. 3(a) and 8(a)).

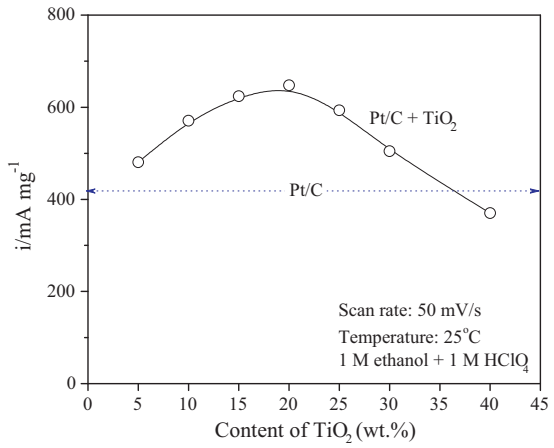

Fig. 9. Peak current of ethanol electro-oxidation on Pt/C + TiO_2 catalysts as a function of TiO_2 content. Specific current *i* is for the current normalized to mass of Pt.

Just like that the TiO_2 particle size can affect the catalyst performance on ethanol electro-oxidation, the content of TiO_2 in the catalyst also has impact on the electro-oxidation of ethanol. Fig. 9 shows the peak current of ethanol electro-oxidation as a function of as-prepared TiO_2 content. From the tendency of the curve we can see that at low contents, the ethanol electro-oxidation is accelerated with increasing the TiO_2 content. However, when TiO_2 content continuingly increased, the Ethanol electro-oxidation will be decelerated instead of accelerated and when the TiO_2 content reaches 40 wt.% the catalyst performs even worse than the pristine Pt/C catalyst. In out experiments, the maximum ethanol electro-oxidation peak current is obtained when the TiO_2 content is 20 wt.%. The whole effect tendency of the TiO_2 content towards ethanol electro-oxidation is understandable just like the case of TiO_2 particle size. When the content is low, there is no large clusters of TiO_2 particles to cut the connection between C particles and the subsequently, the effect of diminishing CO poisoning predominates. However, when the TiO_2 content exceeds the optimum, electron conductivity will be broken by TiO_2 clusters and ethanol electro-oxidation current would be sacrificed.

4. Conclusions

Our studies open a very simple and promising way to enhance the Pt utilization and the activity of traditional Pt/C catalysts for ethanol electro-oxidation in DEFCs by ultrasonically mixing Pt/C catalyst with TiO_2 nanoparticles. Electrochemical measurements confirm that this composite catalyst structure has excellent activity toward ethanol electro-oxidation in which the peak current can be promoted by more than 50% compared to the pristine Pt/C catalyst. Meanwhile, a mechanism that TiO_2 can diminish CO poisoning effect by oxiding the CO intermediates adsorbed on Pt is proposed and verified. In addition, we also highlight that both the TiO_2 particle size and content can impact performances of the composite catalyst and in our experiments, the optimum size and content of TiO_2 nanoparticles are about 10 nm and 20% in weight, respectively.

Acknowledgement

This work was supported by the National Natural Science Foundation of China (20973099) and the Basic Research Program of Shenzhen City (JC201005310703A, JC200903180530A).

References

[1] T. Zhang, Q.M. Wang, J. Power Sources 140 (2005) 72.
[2] R. Dillon, S. Srinivasan, A.S. Arico, V. Antonucci, J. Power Sources 127 (2004) 112.
[3] B.D. Lee, D.H. Jung, Y.H. Ko, J. Power Sources 131 (2004) 207.
[4] S.C.S. Lai, M.T.M. Koper, Phys. Chem. Chem. Phys. 11 (2009) 10446.
[5] S.C. Chang, L.W.H. Leung, M.J. Weaver, J. Phys. Chem. 94 (1990) 6013.
[6] H. Wang, Z. Jusys, R.J. Behm, J. Phys. Chem. B 108 (2004) 19413.
[7] G.A. Camara, T. Iwasita, J. Electroanal. Chem. 578 (2005) 315.
[8] S.C.S. Lai, S.E.F. Kleyn, V. Rosca, M.T.M. Koper, J. Phys. Chem. C 112 (2008) 19080.
[9] J. Shin, W.J. Tornquist, C. Korzeniewski, C.S. Hoaglund, Surf. Sci. 364 (1996) 122.
[10] F. Colmati, G. Tremiliosi-Filho, E.R. Gonzalez, A. Berna, E. Herrero, J.M. Feliu, Faraday Discuss. 140 (2008) 379.
[11] J.F. Gomes, B. Busson, A. Tadjeddine, J. Phys. Chem. B 110 (2006) 5508.
[12] S.C.S. Lai, M.T.M. Koper, Faraday Discuss. 140 (2008) 399.
[13] L. Cao, F. Scheiba, C. Roth, F. Schweiger, C. Cremers, U. Stimming, H. Fuess, L. Chen, W. Zhu, X. Qiu, Angew. Chem. Int. Ed. 45 (2006) 5315.
[14] C. Roth, N. Martz, F. Hahn, J.M. Leger, C. Lamy, H. Fuess, J. Electrochem. Soc. 149 (2002) 433.
[15] C. Roth, N. Benker, Th. Buhrmester, M. Mazurek, M. Loster, H. Fuess, D.C. Koningsberger, D.E. Ramaker, J. Am. Chem. Soc. 127 (2005) 14607.
[16] J. Xi, J. Wang, L. Yu, X. Qiu, L. Chen, Chem. Commun. (2007) 1656.
[17] K.Y. Chan, J. Ding, J.W. Ren, S.A. Cheng, K.Y. Tsang, J. Mater. Chem. 14 (2004) 505.
[18] H.S. Liu, C.J. Song, L. Zhang, J.J. Zhang, H.J. Wang, D.P. Wilkinson, J. Power Sources 155 (2006) 95.
[19] A. Hamnett, Catal. Today 38 (1997) 445.
[20] S.J. Liao, K.A. Holmes, H. Tsaprilis, V.I. Birss, J. Am. Chem. Soc. 128 (2006) 3504.
[21] Y.M. Liang, H.M. Zhang, Z.Q. Tian, X.B. Zhu, X.L. Wang, B.L. Yi, J. Phys. Chem. B 110 (2006) 7828.
[22] E. Reddington, A. Sapienza, B. Gurau, R. Viswanathan, S. Sarangapani, E.S. Smotkin, T.E. Mallouk, Science 280 (1998) 1735.
[23] L.H. Jiang, G.Q. Sun, ZhH. Zhou, ShG. Sun, Q. Wang, ShY. Yan, H.Q. Li, J. Tian, J.S. Guo, B. Zhou, Q. Xin, J. Phys. Chem. B 109 (2005) 8774.
[24] Y.X. Bai, J.J. Wu, J.Y. Xi, J.S. Wang, W.T. Zhu, L.Q. Chen, X.P. Qiu, Electrochem. Commun. 7 (2005) 1087.
[25] M.A. Scibioh, S. Kim, E.A. Cho, T. Lim, S. Hong, H.Y. Ha, Appl. Catal. B: Environ. 84 (2008) 773.
[26] C. Perkins, M. Henderson, C. Peden, G. Herman, J. Vac. Sci. Technol. A 19 (2001) 1942.
[27] K. Drew, G. Girishkumar, K. Vinodgopal, P.V. Kamat, J. Phys. Chem. B 109 (2005) 11851.
[28] E. Antolini, F. Colmati, E.R. Gonzalez, Electrochem. Commun. 9 (2007) 398.
[29] X. Wang, J. Zhang, H. Zhu, Chin. J. Catal. 32 (2011) 74.
[30] A.O. Neto, L.A. Farias, R.R. Dias, M. Brandalise, M. Linardi, E.V. Spinacé, Electrochem. Commun. 10 (2008) 1315.
[31] G. Girishkumar, T.D. Hall, K. Vinodgopal, P.V. Kamat, J. Phys. Chem. B 110 (2006) 107.
[32] E. Frackowiak, G. Lota, T. Cacciaguerra, F. Beguin, Electrochem. Commun. 8 (2006) 129.